

THE IR COUNTERPART TO THE ANOMALOUS X-RAY PULSAR 1RXS J170849–400910¹

G.L. ISRAEL^{2,3}, S. COVINO⁴, R. PERNA⁵, R. MIGNANI⁶, L. STELLA^{2,3}, S. CAMPANA^{4,3}, G. MARCONI⁷, G. BONO², S. MEREGHETTI⁸, C. MOTCH⁹, I. NEGUERUELA¹⁰, T. OOSTERBROEK¹¹, AND L. ANGELINI¹²

1

2. INAF – Osservatorio Astronomico di Roma, V. Frascati 33, I-00040 Monteporzio Catone (Roma), Italy;
gianluca@mporzio.astro.it

3. Affiliated to the International Center for Relativistic Astrophysics

4. INAF – Osservatorio Astronomico di Brera, Via Bianchi 46, I-23807 Merate (Lc), Italy

5. Harvard-Smithsonian Center for Astrophysics, 60 Garden Street, Cambridge, MA 02138, USA

6. European Southern Observatory, Karl-Schwarzschildstr. 2, D-85748 Garching, Germany

7. European Southern Observatory, Casilla 19001, Santiago, Chile

8. CNR-IASF, Istituto di Astrofisica Spaziale e Fisica Cosmica, Sezione di Milano "G.Occhialini", Via Bassini 15, I-20133 Milano, Italy

9. Observatoire de Strasbourg, 11, rue de l'Universite, 67000 Strasbourg, France

10. Dpto. de Física, Ingeniería de Sistemas y Teoría de la Señales, Universidad de Alicante, Apdo. de Correos 99, E03080, Alicante, Spain

11. Space Science Department of ESA, ESTEC, P.O. Box 299, 2200 AG Noordwijk, The Netherlands

12. Laboratory of High Energy Astrophysics, Code 660.2, NASA/Goddard, Space Flight Center, MD 20771, USA

Received: 19 November 2002; Accepted 11 April 2003

ABSTRACT

We report the discovery of the likely IR counterpart to the Anomalous X-ray Pulsar (AXP) 1RXS J170849–400910, based on the combination of *Chandra* HRC-I X-ray position, and deep optical/IR observations carried out from ESO telescopes and the Canada France Hawaii Telescope (CFHT) during 1999–2002. Within the narrow uncertainty region we found two relatively faint ($K'=20.0$ and $K'=17.53$) IR objects. Based on their color and position in the $J-K'$ versus $J-H$ diagram only the brighter object is consistent with the known IR properties of the counterparts to other AXPs. No variability was detected for this source, similarly to what is observed in the case of 4U 0142+614. Like in other AXPs, we found that the IR flux of 1RXS J170849–400910 is higher than expected for a simple blackbody component extrapolated from the X-ray data. If confirmed, this object would be the fourth IR counterpart to a source of the AXP class, and would make the IR excess a likely new characteristic of AXPs.

Subject headings: stars: neutron — stars: pulsars: general — pulsar: individual: — 1RXS J170849–400910 — infrared: stars — X-rays: stars

1. INTRODUCTION

AXPs are thought to be solitary magnetic rotating neutron stars (NSs) either with a standard magnetised field or larger than 10^{14} Gauss (magnetars), although the binary system scenario with a very low mass companion is not completely ruled out by current observational data. (for a review see Israel et al. 2002a; Mereghetti et al. 2002 and references therein). Different production mechanisms for the observed X-ray emission have been proposed, involving either accretion or dissipation of magnetic energy. The magnetar model, originally proposed by Duncan & Thompson (1992) to explain Soft Gamma-ray Repeaters (SGRs), appears to be successful at interpreting most of the properties of AXPs. In fact, AXPs have been linked to SGRs (thought to be magnetars, neutron stars powered by their strong magnetic fields) because of similar timing properties, namely periods and positive period derivatives (Duncan & Thompson 1992; Thompson & Duncan 1993; 1996). What differentiates the two classes of objects is unclear. The similarity in the spin parameters would not be sufficient by itself to differentiate AXPs and SGRs from other groups of pulsars with very different emission properties. Conversely, a very high magnetic field strength (if at all) cannot be the sole factor gov-

erning whether or not a neutron star is a magnetar, a radio pulsar or in a binary system (Camilo et al. 2000).

The possible connection of AXPs with SGRs has gained more credibility with the recent detection of SGR-like X-ray bursts from two AXPs (Kaspi & Gavriil 2002, Gavriil et al. 2002) which also showed IR variability. For 1E 2259+586, IR variability of the likely counterpart has been detected few days after a strong bursting activity seen with the *RXTE* (Kaspi et al. 2002, Israel et al. 2003). Similarly, the variability of the IR counterpart to 1E 1048.1–5937 is thought to be related to X-ray variability (Israel et al. 2002b), though no simultaneous X-ray/IR observations were available. The magnetar scenario does not make any prediction (yet) on the optical/IR emission seen in AXPs. If AXPs are powered by accretion via a disc, in analogy with the X-ray bursts observed in Low Mass X-ray Binaries, it is expected that the effects of the X-ray bursts activity in AXPs (and SGRs) propagate toward longer wavelengths e.g., via reprocessing in the disc (see Middleditch & Nelson 1976; Lawrence et al. 1983). Evidence for flattening (or excess) of the flux distribution in the IR band (with respect to a simple blackbody component forced to be consistent both with the X-ray and optical data) has been reported in three AXPs, namely

¹ The results reported in this Letter are partially based on observations carried out at ESO, La Silla, Chile (63.H-0294, 66.D-0440, 67.D-0116 and 68.D-0350), and the Canada-France-Hawaii Telescope operated by the National Research Council of Canada, the Centre National de la Recherche Scientifique de France and the University of Hawaii (02bf21).

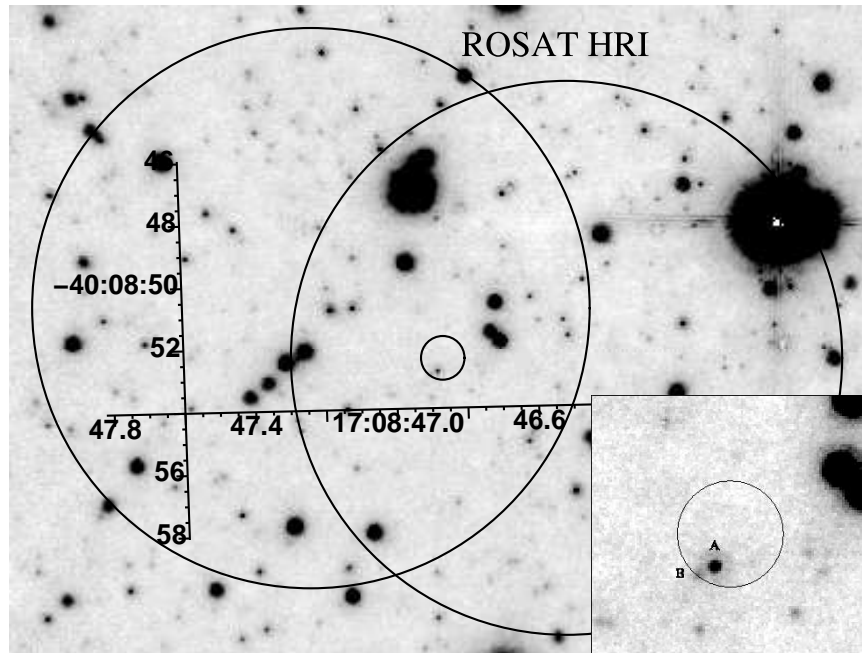


FIG. 1.— Near-IR K' band image of the region including the position of 1RXS J170849–400910, taken from the 3.6-m CFHT. The *ROSAT* and *Chandra* uncertainty circles ($9''$ and $0.8''$, respectively) are also shown. The inset shows the close-up of the *Chandra* position with the two counterpart candidates marked (letter A and B). Coordinates are RA (h m s) and Dec. ($^{\circ}$ ' ' '); equinox J2000).

1E 2259+586, 1E 1048.1–5937 and 4U 0142+614 (Hulleman et al. 2001; Wang & Chakrabarty 2002; Israel et al. 2003). The spectral flattening and variability of the IR emission of AXPs are a potentially important diagnostics for the study of these enigmatic objects and their possible connections with other classes of pulsars.

1RXS J170849–400910 was discovered by the *ROSAT* mission during the All Sky Survey program (Voges et al. 1996), but only a few years later ~ 11 s pulsations were discovered by *ASCA* (Sugizaki et al. 1997). Both the period derivative ($\dot{P} \sim 2 \times 10^{-11}$ s s $^{-1}$) and the optical upper limits inferred for its counterpart were found to be consistent with those of AXPs (Israel et al. 1999). The source is radio quiet (no pulsations detected in the radio band; Israel et al. 2002a) and a stable rotator comparable to radio pulsars (Gavriil & Kaspi 2002). It is also the only AXP for which X–ray spectral variations as a function of the pulse phase have been detected associated to variations of the pulse profile (similar to those observed in “standard” accretion–powered X–ray binary systems; Israel et al. 2003). Finally, 1RXS J170849–400910 represents the only AXP for which a spectral signature, thought to be due to resonant cyclotron absorption, has been detected confirming the presence of a relatively high magnetic field (Rea et al. 2003).

In this paper, we present the results obtained from *Chandra*, ESO and CFHT observations of 1RXS J170849–400910 in the X–ray, optical and IR bands. We identified the likely IR counterpart to this AXP based on positional coincidence and unusual IR colors. The overall (from X–ray to IR) energy distribution is also presented and discussed in the light of the IR excess detected in 1RXS J170849–400910 and other AXPs.

2. *Chandra* OBSERVATIONS

The field of 1RXS J170849–400910 was observed during *Chandra* Cycle 2 with the High Resolution Imager (HRC–I;

Zombeck et al. 1995) on 2001 September 23 for an effective exposure time of 9870 s. Data were reduced with CIAO version 2.2 and analysed with standard software packages for X–ray data (CIAO, XIMAGE, XRONOS, etc.). The observation was carried out with a nominal aspect solution and the latest calibration files were used. Only one source was detected in the HRC–I (see Israel et al. 2002b for details on the detection algorithms). The source has the following coordinates: R.A. = $17^{\text{h}}08^{\text{m}}46^{\text{s}}.87$, DEC. = $-40^{\circ}08'52''.44$ (equinox J2000), with an uncertainty circle radius of $0''.7$ (90% confidence level; consistent with *ROSAT* HRI positions in Israel et al. 1999). Photon arrival times were extracted from a circular region with a radius of $1''.5$, including more than 90% of the source photons, and corrected to the barycenter of the solar system. A coherent pulsation at a period of 11.0011 ± 0.0005 s (90% confidence level) was detected confirming that the source is indeed 1RXS J170849–400910.

We also carried out a spatial profile analysis for the (background subtracted) X–ray emission from a region of $7''$ radius centered on the above reported source position. The spatial profile was found to be in good agreement with the expected *Chandra* Point Spread Function (PSF) for an on–axis source (see Israel et al. 2002b for details). Unfortunately, the high X–ray background level detected in the 1RXS J170849–400910 field prevented a more sensitive search for diffuse emission at larger radii.

3. OPTICAL/IR OBSERVATIONS

Most of the optical/IR data were obtained from the 3.6-m ESO telescope (ESO360; La Silla, Chile) equipped with ESO Faint Object Spectrograph and Camera (EFOSC2; a CCD with 2048×2048 pixels; $0''.157$ pixel scale and $5.2' \times 5.2'$ field of view, FOV) in the optical band, and with the 3.5-m New Technology Telescope (NTT; La Silla, Chile)

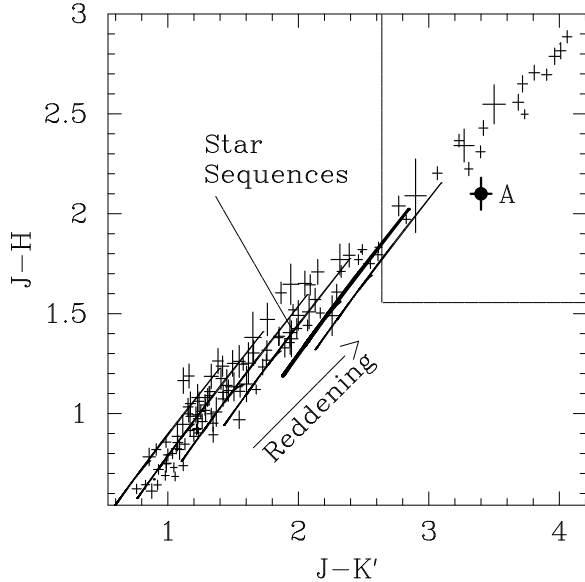


FIG. 2.— Color-color diagram obtained for the objects detected within a radius of $30''$ around the *Chandra* position of 1RXS J170849-400910. The proposed counterpart is marked (A). Star sequences are shown for comparison, for different values of A_V : 0, 2, 4, 6, and 11.2 (thin solid lines; the latter value obtained for the total Galactic absorption), and $A_V=7.8$ (thick solid line; assuming $N_H=1.4\times 10^{22}$ cm^{-2} as inferred from X-ray observations). The rectangle which includes the position of object A represents the most probable region of the diagram where the IR counterpart to 1RXS J170849-400910 would lie, based on the known IR counterparts to AXPs.

equipped with the Son Of Isaac (SOFI; Hawaii HgCdTe 1024×1024 array; $0''.292$ pixel scale and $4.9'\times 4.9'$ FOV) in the near-IR band. Additional IR data were obtained at the 3.6-m CFHT (Mauna Kea, Hawaii) equipped with the Adaptive Optics Bonnette (AOB; Hawaii HgCdTe 1024×1024 array; $0''.035$ pixel scale and $36''\times 36''$ FOV).

Optical Johnson *R* filter deep images were obtained with EFOSS2 on 1999 September 15-16 with effective exposure times of 1500s (seeing of $0''.8$). Standard reduction packages were used in the analysis of the optical data (DAOPHOT II; Stetson 1987) in order to obtain the photometry of each stellar object in the images. A limiting magnitude (3σ confidence level) of $R\sim 26.5$ was reached.

Images in the *J* and *H* bands were initially acquired with SOFI on 2001 May 26 with 1920s (*J*) and 2400s (*H*) of effective exposure time (seeing of $0''.4-0''.6$). Observations yield a limiting magnitude of 22.7 (*J*) and 22.6 (*H*; 3σ confidence level). SOFI *Ks* images were obtained on 2002 February 19 (seeing $0''.8$). The exposure time was of 3000s, and a limiting magnitude of $Ks\sim 21.4$ was reached. In all these cases, single 5 s-long exposure images were taken for each filter with offsets of $40''$ in order to sample and subtract the variable IR background. Finally, *H* and *K'* images were obtained with AOB on 2002 August 17 with effective exposure time of 2700s (for each filter; seeing of $0''.4-0''.5$). Thanks to the adaptive optics we obtained a source PSF of $\sim 0''.12$ yielding a limiting magnitude of 23.1 (*H*) and 21.8 (*K'*). During the latter run single 60s-long exposure images were taken with random offsets in the $4''-10''$ range. Standard IR software packages were used for sky frame subtraction and image coaddition (Eclipse and IRDR; Devillard 1997 and Sabbage et al. 2001).

To register the *Chandra* coordinates of 1RXS J170849-400910 on our optical/IR images, we computed the image astrometry using, as a reference, the positions of stars

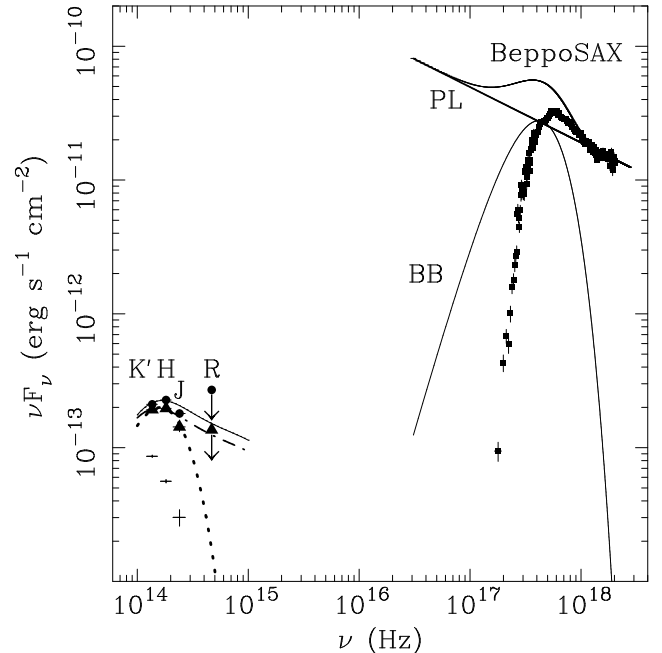


FIG. 3.— Broad band energy spectrum of 1RXS J170849-400910. X-ray raw data are taken from the medium and low energy instruments on board *BeppoSAX* (filled squares) while the solid upper curves are the unabsorbed fluxes for the black body (BB), the power law (PL), and the sum of the two components. On the lower left corner of the plot are the optical/IR fluxes: plus signs are absorbed values, while filled triangles and circles are unabsorbed ones for $A_V=7.8$ and 11.2, respectively. The thick dotted, dash-dotted and solid lines are the fossil disk models discussed in the text.

(about 20 for ESO instruments) selected from the GSC2.2 catalog which has an intrinsic absolute accuracy of about $0''.2-0''.4$ (depending on magnitude and sky position of stars). After taking into account the uncertainties of the source X-ray coordinates ($0''.7$), the rms error of our astrometry ($0''.12$) and the propagation of the intrinsic absolute uncertainties on the GSC2.2 coordinates (we assumed a value of $0''.3$), we estimated the final accuracy to be attached to the 1RXS J170849-400910 position of about $0''.8$. Figure 1 shows a region of $28''\times 20''$ around the 1RXS J170849-400910 position in the *K'* band CFHT image (90% confidence level *ROSAT* and *Chandra* uncertainty circles superimposed). In the inset we show the close-up of the region around the *Chandra* position with the counterpart candidates marked.

The 3.6-m ESO optical *R* band data show that no object is consistent with the *Chandra* position of 1RXS J170849-400910 down to a limiting magnitude of about 26.5. On the other hand, two relatively faint objects are detected in the IR images carried out at the CFHT (marked with A and B in Figure 1). The latter two sources have the following IR magnitudes as inferred from CFHT (NTT) data: $K'=17.53\pm 0.02$, $H=18.85\pm 0.05$ ($Ks=18.3\pm 0.1$, $H=18.6\pm 0.1$ and $J=20.9\pm 0.1$) for object A, $K'=20.00\pm 0.08$ and $H=20.43\pm 0.07$ for B. Unfortunately, no *J* measurement is available for object B due to its faintness and likely confusion with object A in SOFI images.

Figure 2 shows the color-color diagram of the objects in the field with star A marked. Note that the hydrogen column density to 1RXS J170849-400910, inferred from the X-ray observations is $N_H=1.40(6)\times 10^{22}$ cm^{-2} (Israel et al. 2001, Rea et al. 2003), converts into a visual extinction of $A_V \simeq 7.8$ for a typical dust-to-gas ratio (Predehl & Schmitt 1995, see thick solid line in Figure 2). In the *J-K'* versus *J-H* plane the reddening vector lies roughly parallel to the locus of points belonging to star

theoretical isochrones at solar chemical composition and stellar ages ranging from 10 Myr to 8 Gyr (Bono et al. 1997, 2000; a value of 3.1 has been assumed for the parameter $R=A_V/E(B-V)$; Cardelli et al. 1989, Fitzpatrick 1999). We note that the synthetic sequences account for nearly all the objects but few red stars ($J-K'$ colors larger than 3) that are uniformly distributed over the FOV. This is likely due to the parameter R , the value of which is likely larger than that assumed as the “nominal” one (in particular when looking at several spiral arms through the Galactic plane, as in the case of 1RXS J170849–400910). Finally, we used the information on the colors of the known IR counterparts to AXPs ($H-K'=1.1$ and 1.4 for 4U 0142+614 and 1E 1048.1–5937, respectively; Israel et al. 2003; Wang & Chakrabarty 2002), to identify the most probable region of the diagram where the IR counterpart to 1RXS J170849–400910 would lie, if similar colors apply and assuming $A_V \geq 6.5$. Object A is clearly included in the above region and it is also the only object showing unusual colors with respect to both the theoretical star sequences and all other detected objects. All the above results make object A a robust candidate, and in the following we will refer to it as the likely counterpart to 1RXS J170849–400910. Based again on the color, we regard candidate B as a far less likely candidate ($H-K'=0.4$).

4. DISCUSSION

The proposed IR counterpart to 1RXS J170849–400910 is by far the brightest one among those of AXPs: $K'=21.7$, $K'=20.0$, $K_s=19.4$ for 1E 2259+586, 4U 0142+614, and 1E 1048.1–5937, respectively (Hulleman et al. 2001 and 2002, Israel et al. 2003, Wang & Chakrabarty 2002). We note that the relatively large X–ray-to-IR unabsorbed flux ratio of about 500 is lower than that obtained for other AXPs. However, 1RXS J170849–400910 is also the most luminous AXP in the 0.5–10 keV band with an unabsorbed luminosity of $\geq 4 \times 10^{35}$ erg s $^{-1}$ (assuming a distance ≥ 5 kpc). In order to characterize the broadband energy distribution of the source, we plotted the IR through X–ray data of 1RXS J170849–400910 in Figure 3. X–ray fluxes have been inferred by using the phase-averaged spectral parameters obtained with *BeppoSAX* data (Israel et al. 2001, Rea et al. 2003). Two different values of the extinction have been used for model fitting purposes: $A_V=7.8$ and 11.2 (triangles and circles, respectively), corresponding to the N_H inferred from the X–ray spectra and the Galactic absorption in the direction of the source, respectively.

The blackbody component detected in the X–rays ($kT \sim 0.45$ keV; Israel et al. 2001, Rea et al. 2003) cannot account for the (relatively high) IR flux. Similarly, the power-law component, if extrapolated to IR wavelengths, would imply a much higher IR flux level which is simply not observed; a cut-off must therefore occur somewhere in the UV/optical bands. Regardless of the exact position of the cut-off and its origin, we note that the X–ray-to-IR emission of 1RXS J170849–400910 cannot be fit with a simple spectral component (similar to the case of 4U 0142+614 and 1E 2259+586; Hulleman et al. 2000, 2001).

The magnetar model does not account for the observed IR emission or IR variability of AXPs and no predictions can be verified. Therefore, we discuss the above observational findings in the context of models based on fossil disks (Chatterjee et al. 2000; Alpar 2001) since they make clear predictions for the IR emission. However, up to now the latter models are unable to account for the bursts seen in AXPs and SGRs.. In the case of

a fossil disk the IR emission arises mainly from two components: viscous dissipation and reprocessing of X–ray flux impinging on the disk from the pulsar (Perna et al. 2000, Perna & Hernquist 2000, Alpar 2001). Specifically, at IR wavelengths and based on the X–ray luminosity of 1RXS J170849–400910, the dominant emission component is expected to be X–ray irradiation. The models we considered have been computed for a distance of 5 kpc and the observed X–ray luminosity as an input parameter, but since the disk luminosity scales almost linearly with the X–ray luminosity, the result is nearly independent of the distance. As far as the X–ray spectrum, in the accretion model (with magnetic fields of $\sim 10^{12}$ Gauss) one would expect the emission to be roughly a blackbody produced in a region (polar cap) much smaller than the area of the star. Current X–ray data are consistent with this, but not good enough to allow a firm discrimination with respect to the X–ray spectrum of a magnetar, in which case one would expect the area of the emitting region to be consistent with the whole surface of the star (Perna et al. 2001).

In Figure 3 we show disk models obtained with the inner and outer radius of the disk, r_{in} and r_{out} , and the inclination left free to vary (however, note that the inclination only scales the fluxes, while r_{in} and r_{out} modify the shape of the model and the flux peak position; see Perna et al. 2000 for details). The best fit was obtained for a small truncated disk, with r_{in} and r_{out} equal to 10^{11} and 5×10^{11} cm, respectively (dotted line in Figure 3). However, this solution would not be able to explain the X–ray emission from AXPs, being the value of r_{in} larger than the corotation radius ($\sim 8 \times 10^9$ cm), the characteristic value of r_{in} in order to have accretion on the neutron star surface, and at the same time, spin-down. Therefore, we fixed r_{in} to the corotation radius for two different values of extinction. The results of the fit are shown in Figure 3 (dashed-dotted and solid lines, respectively). Values of $r_{out}=10^{12}$ and 8×10^{11} cm were obtained for $A_V=7.8$ and 11.2 , respectively, (fallback compact disks; Menou et al. 2001). In both cases the J measurement is lower than the model expectations (2σ). The above solution might be applied also to the case of an accretion disk formed by mass transfer from a (light) companion, although in this case an (unknown) amount of IR flux should be originated also from the star surface. We note that IR flattening has been recently discovered also for 4U 0142+614, and likely during an X–ray bursting activity phase of 1E 1048.1–5937 (Wang & Chakrabarty 2002, Israel et al. 2003). The IR flattening or excess might represent a new important property shared by AXPs.

The IR emission of AXPs in the magnetar scenario, remains to be addressed through detailed modeling. However, we note that the presence of a disk would not be necessarily in contrast with the magnetar scenario. Three AXPs are associated with supernova remnants and likely embedded in dense regions. Therefore a “hybrid” scenario in which a magnetar irradiates a fossil disk (the matter of which is not accreting in this case) might not be unreasonable, though it should be confirmed through additional future observations and its consistency checked through theoretical studies.

In conclusion, even though we propose a possible solution for the IR excess observed in AXPs, we note that none of the proposed theoretical models (at least in their present form) seem to be able to easily account simultaneously for the IR, optical and X–ray emission of AXPs.

This work is supported through CNAA, ASI, CNR and

Ministero dell'Università e Ricerca Scientifica e Tecnologica (MURST-COFIN) grants. The authors thank Olivier Hainaut, Leonardo Vanzi and the NTT Team for their kind help during

ESO observations. We also thank Olivier Lai and the CFHT team for their support. We finally thanks Hank Donnelly of the *Chandra* Team.

REFERENCES

- Alpar, M.A. 2001, ApJ, 554, 1245
 Bono, G., Caputo, F., Cassisi, S., Castellani, V., Marconi, M. 1997, ApJ, 479, 279
 Bono, G., Caputo, F., Cassisi, S., Marconi, M., Piersanti, L., Tornambé, A. 2000, ApJ, 543, 955
 Camilo, F., Kaspi, V. M., Lyne, A. G., Manchester, R. N., Bell, J. F., D'Amico, N., McKay, N. P. F., & Crawford, F. 2000, ApJ, 541, 367
 Cardelli, J. A., Clayton, G. C., & Mathis, J. S. 1989, ApJ, 345, 245
 Chatterjee, P., Hernquist, L., & Narayan, R. 2000, ApJ, 534, 373
 Devillard, N. 1997, The Messenger, 87
 Duncan, R. C. & Thompson, C. 1992, ApJ, 392, L9
 Fitzpatrick, E. L. 1999, PASP, 111, 63
 Gavriil, F. P. & Kaspi, V. M. 2002, ApJ, 567, 1067
 Gavriil, F. P., Kaspi, V. M., & Woods, P. M. 2002, Nature, 419, 142
 Hulleman, F., van Kerkwijk, M. H., & Kulkarni, S. R. 2000, Nature, 408, 689
 Hulleman, F., Tennant, A. F., van Kerkwijk, M. H., Kulkarni, S. R., Kouveliotou, C., & Patel, S. K. 2001, ApJ, 563, L49
 Israel, G.L., Covino, S., Stella, L., et al. 1999, ApJ, 518, L107
 Israel, G.L., Oosterbroek, T., Stella, L., et al. 2001, ApJ, 560, L65
 Israel, G.L., Mereghetti, S., & Stella, L. 2002a, in γ -Ray Bursts in the Afterglow Era, ed. S. Mereghetti & M. Feroci, Mem.S.A.It., Vol. 73, N. 2, pag. 465 (see also astro-ph/0111093)
 Israel, G.L., Covino, S., Stella, L., et al. 2002b, ApJ, 580, L143
 Israel, G.L., et al. 2003, in preparation
 Kaspi, V.M., Gavriil, F.P., & Woods, P.M. 2002, IAU Circ., 7926
 Kaspi, V.M. & Gavriil, F.P. 2002, IAU Circ., No. 7924
 Lawrence, A. et al. 1983, ApJ, 271, 793
 Menou, K., Perna, R., & Hernquist, L. 2001, ApJ, 559, 1032
 Mereghetti, S., Chiarlone, L., Israel, G. L., & Stella, L. 2002, in Neutron Stars, Pulsars and Supernova Remnants, eds. W. Becker, H. Lesch & J. Trümper (Garching: MPE), in press (astro-ph/0205122)
 Middleditch, J. & Nelson, J. 1976, ApJ, 208, 567
 Perna, R., Hernquist, L., & Narayan, R. 2000, ApJ, 541, 344
 Perna, R. & Hernquist, L. 2000, ApJ, 544, L57
 Perna, R., Heyl, J.S., Hernquist, L.E., Juett, A.M., Chakrabarty, D. 2001 ApJ, 557, 18
 Predehl, P. & Schmitt, J. H. M. M. 1995, A&A, 293, 889
 Rea, N., Israel, G. L., Stella, L., et al. 2003, ApJ, 586, L65
 Sabbey, C. N., McMahon, R. G., Lewis, J. R., & Irwin, M. J. 2001, ASP Conf. Ser. 238: Astronomical Data Analysis Software and Systems X, 10, 317
 Sugizaki, M., Nagase, F., Torii, K., et al. 1997, PASJ, 49, L25
 Stetson, P.B., 1987, PASP, 99, 191
 Thompson, C., & Duncan, R. C. 1993, ApJ, 408, 194
 Thompson, C., & Duncan, R. C. 1996, ApJ, 473, 322
 Voges, W., Aschenbach, B., Boller, T., et al. 1996, IAU Circ.6420
 Wang, Z.-X. & Chakrabarty, D. 2002, ApJ, 579, L33
 Zombeck, M.V., Chappell, J.H., Kenter, A.T., Moore, R.W., Murray, S.S., Fraser, G.W., & Serio, S. 1995, Proc. SPIE, 2518, 96